Strain-Driven Alloying in Ge/Si(100) Coherent Islands

S. A. Chaparro,[1] Jeff Drucker,[1,2,*] Y. Zhang,[1] D. Chandrasekhar,[3] M. R. McCartney,[3] and David J. Smith[3,4]
[1]*Materials Research Institute, The University of Texas at El Paso, El Paso, Texas 79968-0515*
[2]*Physics Department, The University of Texas at El Paso, El Paso, Texas 79968-0515*
[3]*Center for Solid State Science, Arizona State University, Tempe, Arizona 85287*
[4]*Department of Physics and Astronomy, Arizona State University, Tempe, Arizona 85287*
(Received 22 March 1999)

Ge/Si(100) island size distributions were monitored for coverages between 3.5 and 14.0 monolayers at growth temperatures from 450 to 600 °C. Features in these distributions are correlated with characteristic island morphologies. The mean dome cluster size increased and the onset of island dislocation was delayed as the growth temperature increased. At 600 °C, very large hut clusters are formed. This behavior is attributed to strain-assisted alloying of the Ge clusters. Energy dispersive x-ray analysis confirms Si diffusion into the Ge clusters at 600 °C. An atomistic elastic model supports the interpretation that alloying is driven by strain energy enhancement near the island perimeters.

PACS numbers: 68.55.–a, 68.35.Bs, 68.35.Dv, 68.35.Fx

Self-assembled quantum dots (SAQD) in heteroepitaxial semiconductor systems have been an area of recent intense study. These SAQD systems provide a straightforward route for fabrication of nanostructures with relatively uniform size and shape. It has been predicted [1] that size uniformity throughout the dot ensemble will optimize their performance in possible device applications. To achieve this uniformity, the substrate temperature T, deposition rate, and coverage θ may be varied. Previously, we reported that higher growth temperatures can narrow the width of Ge/Si(100) island size distributions [2]. Until recently [3], it has been tacitly assumed that alloying may be unimportant for SAQD formation. Here, we report results from a systematic variation of T and θ which show that Si readily diffuses into Ge clusters for $T \geq 550$ °C. This alloying results in an increased mean dome cluster (truncated pyramids bound by {210} and {311} facets) size and delayed defect formation with increasing growth temperature. Further, we find that quite large hut clusters (clusters bound by {510} facets) exist for $T = 600$ °C.

Most other investigations of Ge-Si interdiffusion have involved planar heterostructures and prolonged anneals [4–10]. Kamins [11] showed that 650 °C annealing can reverse the hut-to-dome transition commonly observed during Ge/Si coherent island evolution. Our investigation, on the other hand, demonstrates that intermixing occurs on the time scale of minutes during Ge/Si coherent islanding. This alloying alters the misfit, changing the size range over which various island morphologies may exist [12]. Further, by altering misfit and concentration, the band offsets [13], confinement potentials, and, ultimately, the optoelectronic properties may be affected.

The samples were grown by standard molecular beam epitaxy techniques by depositing pure Ge onto Si(100). Further details are presented elsewhere [2]. All samples were prepared at growth rates of 1.4 ML/min (1 ML = 6.78×10^{14} atoms/cm^2) using substrate temperatures of either 450, 550, or 600 °C. At each T, θ ranged from 3.5 to 14.0 ML in 1.5-ML increments. Sample morphology was determined by *ex situ* atomic force microscopy (AFM). Our samples are rectangular strips cleaved from Si wafers with the long axis parallel to $\langle 110 \rangle$. Orienting this long axis parallel to the x-scan direction in all AFM images allowed convenient identification of surface crystallographic features. AFM cross-sectional analysis identified facet contact angles, allowing the island classifications discussed below. Statistically significant island size distributions were obtained by imaging large areas of each sample. Plan-view imaging of selected samples with transmission electron microscopy (TEM) identified the critical size for dislocation formation, and energy-dispersive x-ray nanoanalysis (EDX) was used for nm-scale composition determination.

The size distributions in Fig. 1 plot the number of islands/cm^2 vs the island diameter for each of the three growth temperatures. Although the islands do not have a circular base, we use the diameter $d = 2\sqrt{A/\pi}$ as a convenient measure of their size. Within each distribution, a range of coverages is displayed. Analysis of clusters within the peak at the smallest diameter indicates that they correspond either to huts [14–16] or pyramids [17]. This peak position is unchanged, within the accuracy of AFM, as the growth temperature increases. The largest diameter peak for all three temperatures corresponds to dome clusters [14,16]. Note that the dome peak shifts to larger island sizes as the growth temperature increases. For example, at $\theta = 9.5$ ML, the average dome diameter is 39, 65, and 80 nm at $T = 450$, 550, and 600 °C, respectively. Moreover, as we previously reported [2], the normalized width of the dome peak decreases as the growth temperature increases. $\sigma_d/\langle d \rangle = 0.17$ at 450 °C, 0.11 at 550 °C, and 0.08 at 600 °C (σ_d = standard deviation of island diameter and $\langle d \rangle$ = mean island diameter).

At 600 °C, a peak between the hut and dome peak is evident which is absent at lower temperatures. Analysis

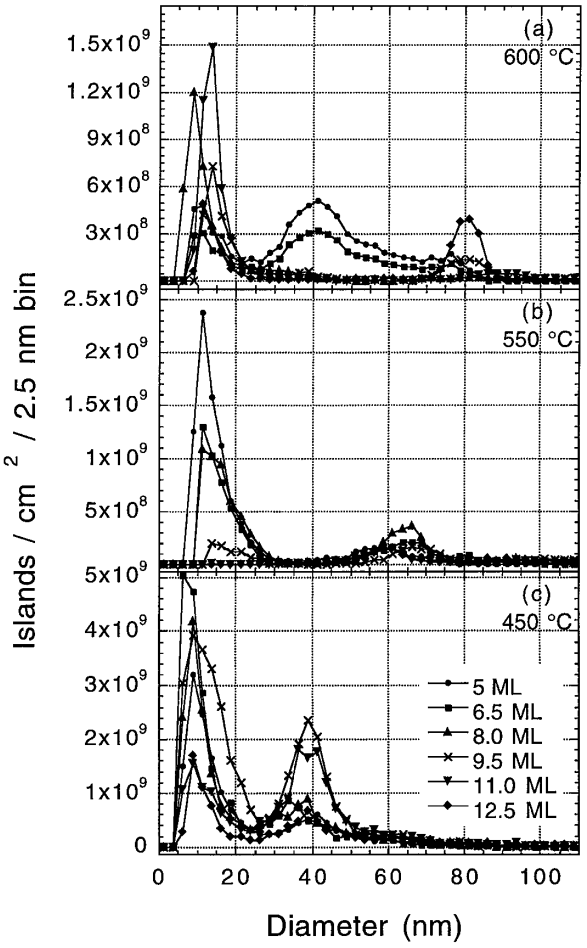

FIG. 1. Island size distributions for selected coverages at the indicated growth temperatures.

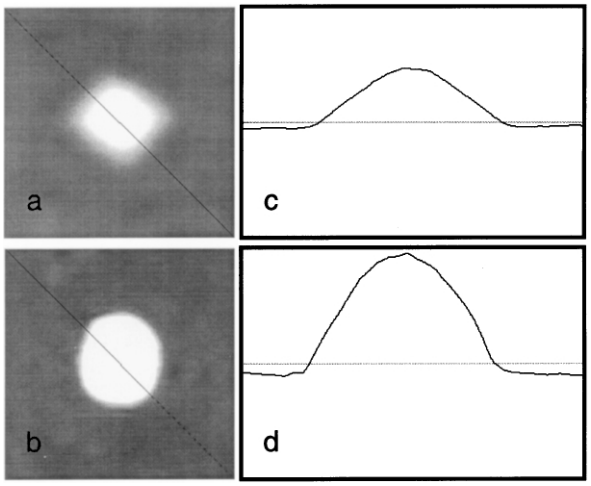

FIG. 2. 125 nm^2 AFM images and cross sections along the indicated line of a large hut grown at 600 °C [(a) and (c)] and a dome grown at 450 °C [(b) and (d)]. The line scan frames are 100 nm × 18 nm. The base width in (c) is as large as (d) but the 11.5° contact angle shows it is a pyramid.

of clusters within this peak indicates that they are morphologically similar to huts. They are bound by {510} facets although their diameters are in the range of those observed for domes formed at 450 °C. Figure 2 displays a cross section of one of these large huts grown at 600 °C and a dome of the same size grown at 450 °C. For a range of coverages at 600 °C, these large huts may coexist with both the smaller huts with $d \leq 25$ nm and the domes with 70 nm $\leq d \leq$ 90 nm. As discussed below, we attribute the existence of the large huts to Ge/Si alloying. This interpretation is consistent with the observation that the characteristic size of various cluster morphologies scales inversely with the square of the misfit [12,18].

For each temperature, a tail extending to very large diameters is evident on each dome peak. Islands within this tail correspond to the super domes observed by Williams [19] and dislocated islands observed by Krishnamurthy [20]. These clusters are morphologically similar to the coherent dome clusters at smaller sizes. However, plan-view TEM analysis clearly showed that all clusters in this tail contained defects such as dislocations and stacking faults, whereas islands within the huts, big huts, and dome peaks generally remained coherent. Thus, once dislocations are formed, the overall island size distribution broadens dramatically. This confirms that the chemical potential of an island reduces upon dislocation resulting in rapid growth [21]. Our plan-view TEM observations confirm that the onset of island dislocation corresponds to the large diameter edge of the dome peak. Thus, we observe that the minimum size of dislocated islands rises with increasing growth temperature, i.e., $d_c = 50$, 70, and 90 nm at $T = 450$, 550, and 600 °C, respectively.

Figure 3 displays a dark-field scanning transmission electron micrograph (STEM) and EDX line scan taken along the indicated line as obtained with a Philips CM200 field emission electron microscope. The island in Fig. 3 is a large dome grown at 600 °C. The line scans display the integrated counts for the Ge-L and Si-K peaks along the line and are not absorption or background corrected. Within the ~0.5 nm resolution of EDX, the Ge intensity falls abruptly to background levels at the substrate while the Si intensity remains significantly above background well into the Ge island.

Our observations that the mean dome radius, and the minimum radius for dislocation formation, both increase with growth temperature, and the appearance of very large hut clusters at 600 °C, are consistent with Ge-Si alloying. Early analytical treatments of coherent islanding [22,23] identified a critical size for island dislocation analogous to the critical thickness for dislocation of strained layers. This critical size increases as misfit decreases for fixed island shape. Thus, our observation that dislocation introduction is delayed as the growth temperature increases is consistent with alloying and its concomitant misfit reduction. The increase in the mean dome cluster size with growth temperature is

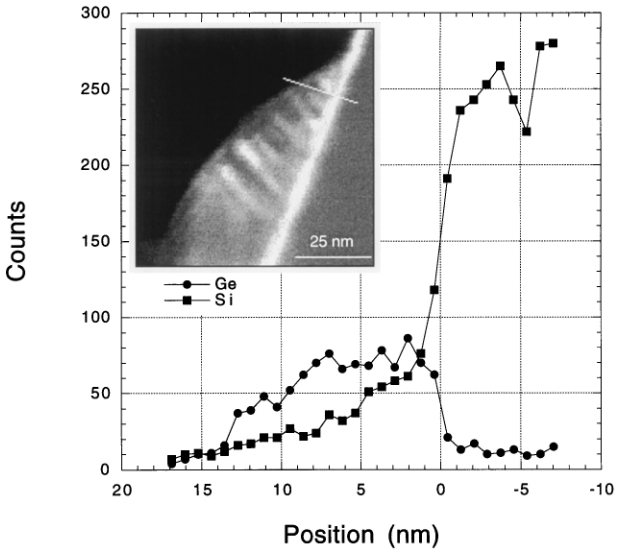

FIG. 3. Dark field STEM image and EDX line scan along the indicated line of a dome grown at 600 °C. Within the ~0.5 nm EDX resolution, the Ge-L intensity falls abruptly to background levels in the substrate. The Si-K intensity remains above background well into the Ge cluster demonstrating that Si diffuses into the Ge island at 600 °C.

also indicative of Ge-Si intermixing within the context of Schukin's model [18] for the equilibrium size of coherent islands. Qualitatively, Schukins' model predicts that the balance between facet, edge, and strain energies determines the preferred size for coherent islands. Thus, as alloying decreases the misfit, this preferred size should increase in agreement with our observations.

In order to gain further insight into the existence of alloyed domes at 550 and 600 °C and very large huts at 600 °C, but not lower temperatures, we consider a simple linear elastic model of coherent islands. Upon a simple cubic substrate of lattice constant a, a simple cubic film of lattice constant $a(l + \varepsilon)$ is placed. Nearest (NN) and next-nearest (NNN) neighbor atoms interact harmonically so that the total elastic energy of the system is given by

$$E_{\mathrm{el}} = \tfrac{1}{2} \sum_{i=\mathrm{all\ atoms}} \sum_{j=\mathrm{NN,NNN}} \tfrac{1}{2} k_{ij} \left(\frac{\Delta l_{ij}}{l_{ij}^{o}} \right)^2 . \quad (1)$$

k_{ij} is the force constant (for the results presented here, $k_{\mathrm{NN}} = k_{\mathrm{NNN}}$) and $\Delta l_{ij} = l_{ij} - l_{ij}^{o}$ with l_{ij}^{o} being the relaxed bond length between atoms i and j. Equation (1) is equivalent to summing the product of the stress and strain tensors over the entire crystal volume. The film comprises three atomic layers and a square-based pyramid whose base is aligned along $\langle 100 \rangle$. Periodic boundary conditions in the growth plane are employed and the substrate bottom is a free boundary. The pyramid base width is no larger than $1/2$ of the substrate width. Thus, the interpyramid spacing is at least twice the base width [24]. Initially, all atoms occupy substrate atom positions and a conjugate gradient method is used to relax the structure finding the atomic positions minimizing the total elastic energy (1).

Figure 4 displays plots of the substrate and film atom interfacial elastic energies using $E_{\mathrm{site}} = \frac{1}{2} \sum_{\mathrm{NN,NNN}} k(\Delta l/l^{o})^2$ for pyramids of 80-atom side-length lying on a substrate which is 160 atoms wide and 80 atoms deep with a 3-atom thick wetting layer. (a) and (b) are for 15° and (c) and (d) are for 45° contact angles. (a) and (c) show the bottommost film atoms and (b) and (d) show the topmost substrate atoms. Darker grays correspond to higher elastic energy densities. These plots are for a 5% misfit. Each image is scaled so that black represents the highest and white the lowest energy density within that image. Clearly, the energy densities are largest near the pyramid perimeter. This elastic energy concentration at the cluster boundary has been found by other authors [25,26] who have discussed its effects on coherent island growth, however, they have tacitly assumed that it is unimportant in driving Si-Ge intermixing as we discuss here.

Figure 5 plots the scaled elastic energy density at the film/substrate interface for atoms in the elastic energy maximum near the island perimeter along the $\langle 100 \rangle$ and $\langle 110 \rangle$ directions. The scaled elastic energy density for a film (substrate) interface atom is the value of the elastic energy density for that atom divided by the elastic energy of a film (substrate) atom for a 3 ML uniform film. Thus, Fig. 5 plots the enhancement of the interfacial elastic energy density for atoms near the island perimeter. This enhancement is due to the stress concentration at the

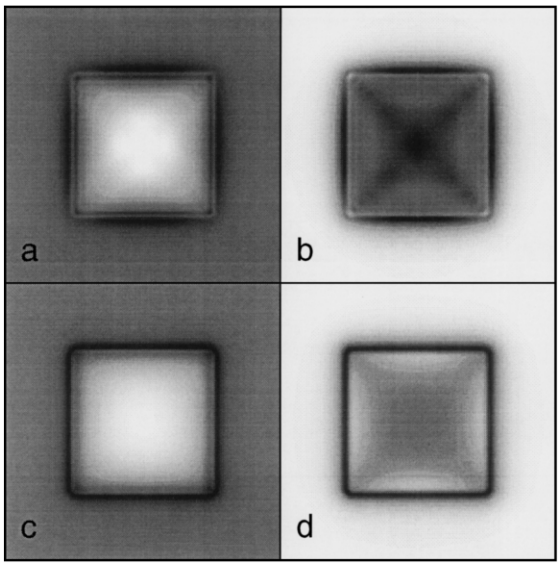

FIG. 4. Gray-scale plots of the site elastic energy for the bottommost film atoms, (a) and (c), and the topmost substrate atoms, (b) and (d), for pyramid clusters. Darker grays correspond to higher energies. Each plot is scaled so that black is the highest and white the lowest energy in that image. (a) and (b) are for 15° and (c) and (d) are for 45° contact angles.

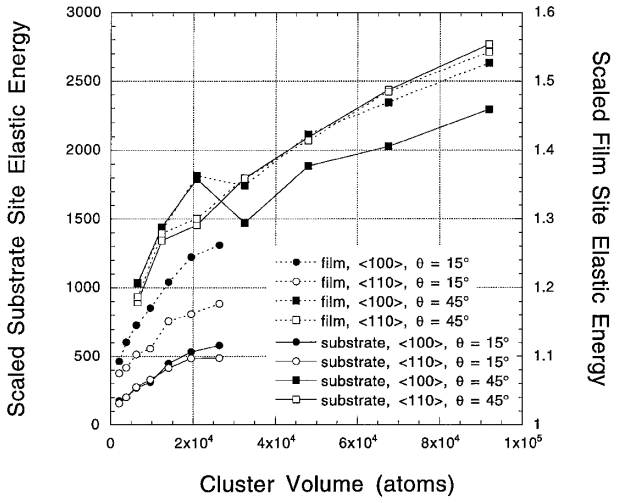

FIG. 5. The scaled elastic energy density vs island volume for sites within the maximum near the cluster perimeter evident in Fig. 4. Points along the indicated crystal directions are plotted for each island volume. The scaled elastic energy density for a substrate (film) site is the quotient of the site elastic energy and the substrate (film) interface elastic energy of a 3 ML thick uniform film.

island perimeter and is relative to that of a planar 3 ML thick layer.

The rise of this scaled elastic energy density with increasing cluster volume is significant. Diffusion should be enhanced in regions with high elastic energy density. Several investigations of diffusion in strained SiGe heterostructures have indicated enhanced intermixing as strain rises [5–7,9,10]. Thus, Figs. 4 and 5 allow us to further explain our results. First, our observation that domes alloy at lower temperatures than huts is consistent with the scaled elastic energy density being larger at the perimeter of pyramids with steeper contact angles. The existence of large, alloyed pyramids only at 600 °C and not at lower growth temperatures is also a consequence of the rise in the scaled elastic energy density. These alloyed huts exist only at the highest growth temperature investigated since lower temperatures are not sufficient to activate intermixing. These lower temperatures are sufficient, however, to activate intermixing of the domes due to the higher elastic energy density at their boundaries. We also briefly note that this simple elastic model explains the composition inhomogeneity observed by Kamins [11] in alloyed domes. They found that the Si concentration was enhanced at the boundary of alloyed dome clusters, precisely where we predict the degree of intermixing should be largest.

Recently, Tersoff [3] has proposed that the free-energy barrier for nucleation of coherently strained alloy (i.e., SiGe) islands on a planar alloy layer, may be significantly lowered by segregation of the high misfit component to the island. His model indicates that no barrier reduction is possible for pure (i.e., Ge islands formed on a pure Ge layer) islands. Our observation that the hut peak in Figs. 1(a)–1(c) is invariant with respect to growth temperature supports Tersoff's prediction. Huts alloy only *after* they have existed for some time after nucleating. Interestingly, the sharpness of the dome peak in Figs. 1(a)–1(c) suggests that there is a temperature-dependent equilibrium concentration for dome clusters. That is, if there were a range of concentrations throughout the dome ensemble, we would expect the dome peak to broaden subsequent to alloying rather than narrowing as our evidence indicates.

This work was supported by the National Science Foundation through Grants No. DMR 9496296, No. 9724305, and No. 9840310. We also acknowledge use of the Center for High Resolution Electron Microscopy at Arizona State University.

*jdrucker@utep.edu

[1] K. Vahala, IEEE J. Quantum Electron. **24**, 523 (1988).
[2] J. Drucker and S. A. Chaparro, Appl. Phys. Lett. **71**, 614 (1997).
[3] J. Tersoff, Phys. Rev. Lett. **81**, 3183 (1998).
[4] G. L. McVay and A. R. DuCharme, J. Appl. Phys. **44**, 1409 (1973).
[5] S. Chang *et al.*, Appl. Phys. Lett. **54**, 1253 (1989).
[6] J.-M. Baribeau, R. Pascual, and S. Saimoto, Appl. Phys. Lett. **57**, 1502 (1990).
[7] S. M. Prokes, O. J. Glembocki, and D. J. Godbey, Appl. Phys. Lett. **60**, 1087 (1992).
[8] D. A. Grutzmacer *et al.*, Appl. Phys. Lett. **63**, 2531 (1993).
[9] N. Cowern *et al.*, Phys. Rev. Lett. **72**, 2585 (1994).
[10] K. Shum, P. M. Mooney, and J. O. Chu, Appl. Phys. Lett. **71**, 1074 (1997).
[11] T. I. Kamins *et al.*, Appl. Phys. A **67**, 1 (1998).
[12] J. Floro *et al.*, Phys. Rev. Lett. **79**, 3946 (1997).
[13] C. Van de Walle and R. M. Martin, Phys. Rev. B **34**, 5621 (1986).
[14] G. Medeiros-Ribeiro, A. M. Bratkovski, and R. S. Williams, Science **279**, 353 (1998).
[15] Y. W. Mo *et al.*, Phys. Rev. Lett. **65**, 1020 (1990).
[16] M. Tomitori *et al.*, Appl. Surf. Sci. **76/77**, 322 (1994).
[17] G. Medeiros-Ribeiro *et al.*, Phys. Rev. B **58**, 3533 (1998).
[18] V. Schukin *et al.*, Phys. Rev. Lett. **75**, 2968 (1995).
[19] R. S. Williams *et al.*, J. Phys. Chem. **102**, 9605 (1998).
[20] M. Krishnamurthy, J. Drucker, and J. A. Venables, J. Appl. Phys. **69**, 6461 (1991).
[21] J. Drucker, Phys. Rev. B **48**, 18 203 (1993).
[22] N. Cabrera, Surf. Sci. **2**, 320 (1964).
[23] W. A. Jesser and D. Kulhmann-Wilsdorf, Phys. Status Solidi **19**, 95 (1967).
[24] Empirically, we determined closer spacings lead to elastic interactions which invalidate our conclusions.
[25] H. Dobbs *et al.*, Phys. Rev. Lett. **79**, 897 (1997).
[26] D. Jesson *et al.*, Phys. Rev. Lett. **80**, 5156 (1998).